

# LOW-LYING STRUCTURE OF ${}^6\text{He}$ STUDIED BY THE ${}^6\text{Li}(t, {}^3\text{He}){}^6\text{He}$ REACTION

T. Nakamura<sup>a</sup>, T. Aumann<sup>b</sup>, D. Bazin, Y. Blumenfeld<sup>c</sup>, B.A. Brown, J. Caggiano<sup>d</sup>, R. Clement, T. Glasmacher, P.A. Lofy, A. Navin<sup>e</sup>, B.V. Pritychenko, B.M. Sherrill, J. Yurkon

Low-lying excitations of weakly-bound nuclei have raised intriguing issues. For the weakly-bound nucleus  ${}^6\text{He}$ , which has a peculiar "Borromean" structure, soft dipole excitation and a three-body  $2^+$  resonance have been predicted [1, 2, 3]. Recently, the soft dipole transition has indeed been reported in the  ${}^6\text{Li}({}^7\text{Li}, {}^7\text{Be}){}^6\text{He}$  reaction [4], which may indicate the existence of low-lying intruder states. The independent study with the same reaction [5] indicated, however, that this low-lying structure was a  $2^+$  resonance. Hence, the detailed experiment to clarify the low-lying structure of  ${}^6\text{He}$  has been called for. Here we report the study of  ${}^6\text{He}$  by the  ${}^6\text{Li}(t, {}^3\text{He}){}^6\text{He}$  reaction. The  $(t, {}^3\text{He})$  reaction has recently been proven to be a powerful spectroscopic tool where a secondary triton beam is combined with a high resolution spectrograph [6, 7].

The experiment was performed using the S800 spectrograph. The secondary triton beam had a typical intensity of about  $10^6$  particles/s, a mean energy of 336 MeV. It was used to bombard a  ${}^6\text{Li}$  target with a thickness of  $17.4 \text{ mg/cm}^2$  (95% enriched). The momentum of the outgoing  ${}^3\text{He}$  ion was measured by the spectrograph operated in dispersion matching mode. The detailed description of the experiment has been published elsewhere [8].

Fig. 1 shows the energy spectra obtained for the  ${}^6\text{Li}(t, {}^3\text{He}){}^6\text{He}$  reaction at the  $0^\circ$  (a) and  $8^\circ$  (b) settings of the S800. Besides the conspicuous peaks for the transitions to the ground and first excited states in  ${}^6\text{He}$ , the spectra show the strong and broad structures at  $E_x \sim 5 \text{ MeV}$  and  $\sim 15 \text{ MeV}$ . The structure around 15 MeV is notable at the higher angular setting, while the structure around 5 MeV rapidly decreases as  $\theta_{\text{lab}}$  increases. An interesting feature of the 5 MeV bump is its very asymmetric shape.

The spectral shape from the 0 degree setting (Fig. 1(a)) was analyzed by Gaussian peak-fitting. The asymmetric structure around 5 MeV was decomposed into three Gaussians to better study the nature of its components. This division is arbitrary, although at least three Gaussians are necessary to obtain an overall agreement of this structure, indicating its complex composition. The best fit values for the locations of three Gaussians were  $4.4 \pm 0.1 \text{ MeV}$ ,  $7.7 \pm 0.2 \text{ MeV}$  and  $9.9 \pm 0.4 \text{ MeV}$ , respectively. The structure around 15 MeV was best fitted with a location of  $14.6 \pm 0.2 \text{ MeV}$ .

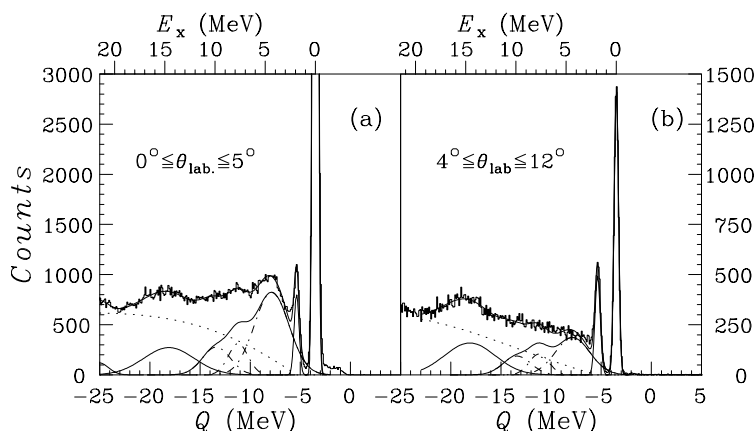


Figure 1: Energy spectra for the  ${}^6\text{Li}(t, {}^3\text{He}){}^6\text{He}$  reaction measured at 336 MeV for (a) 0 degree setting of the S800 ( $0^\circ - 5^\circ$ ), and (b) 8 degree setting ( $4^\circ - 12^\circ$ ).

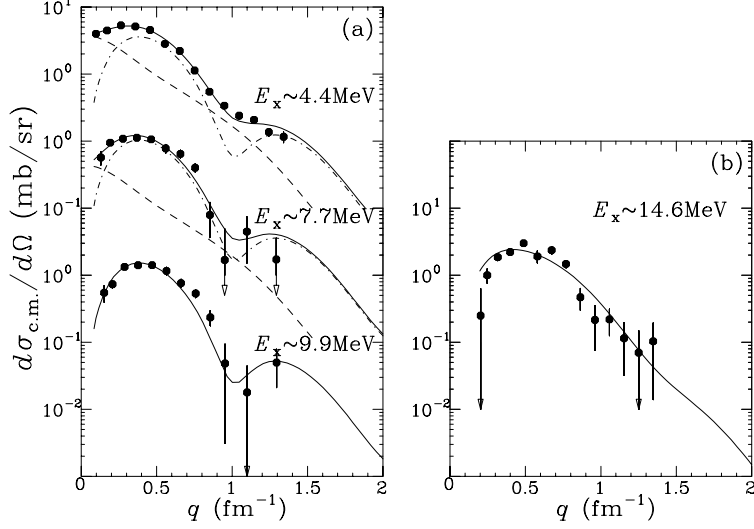


Figure 2: Differential cross sections for the 5 MeV (4.4, 7.7 and 9.9 MeV components) and 14.6 MeV structures. Solid curves show the results of DWBA calculations. The contributions from the negative- and positive-parity states are shown by the dot-dashed and dashed curves, respectively, for 4.4 and 7.7 MeV components. The 9.9 and 14.6 MeV components are described by the transition purely to the negative-parity states.

Differential cross sections as a function of momentum transfer  $q$  are shown in Fig. 2(a) for the 5 MeV structure (4.4, 7.7, and 9.9 MeV components) and in Fig. 2(b) for the 15 MeV (14.6 MeV) structure. Distorted Wave Born Approximation (DWBA) calculations were performed with the computer code DW81 [9]. Optical-model parameters of a Woods-Saxon shape were extracted from our elastic scattering measurement of  ${}^3\text{He}$  on  ${}^6\text{Li}$ . The effective projectile-nucleon ( $t$ - $N$ ) interactions were based on the effective  ${}^3\text{He}$ - $N$  interactions derived phenomenologically for the ( ${}^3\text{He}, t$ ) reaction by Van der Werf *et al.* [10]. The wave functions and one-body transition densities for the input for DW81 were calculated with the shell-model computer code OXBASH [11, 12, 13]. The detail of  ${}^6\text{He}$  energy levels from this shell-model calculation is discussed elsewhere [8].

As shown in Fig. 2(a), the angular distributions for three components for 5 MeV structure all follow the characteristics of  $\Delta L=1$  transition (dot-dashed curve), indicating the existence of low-lying dipole states in  ${}^6\text{He}$ . On the other hand, the cross section at  $q \sim 0$  for the 4.4 MeV region is larger than for the 7.7 MeV and 9.9 MeV regions, suggesting that the structure has a small  $\Delta L=0,2$  component at the lower excitation energies. Indeed, the best agreement is obtained with an admixture of transitions to negative parity states ( $\Delta L=1$ ), with those to the positive-parity states ( $\Delta L=0,2$ ) being only at lower excitation energies.

The angular distribution for the 15 MeV structure is shown in Fig. 2(b). The distribution is broader than those for the 5 MeV structure. The distribution is well reproduced assuming that the transition occurs to the predicted negative parity states ( $\Delta L=1$ ) at  $E_x \sim 16$ – $20$  MeV. The difference between the  $\Delta L=1$  transitions to the 5 MeV and 15 MeV structures is that the former is dominated by a transition to  $2s1p^{-1}$  (proton hole in the  $1p$  orbital and neutron in  $2s$  orbital in  ${}^6\text{Li}$ ), while the latter is dominated by the transition to  $1p1s^{-1}$  and  $1d1p^{-1}$  configurations. The difference of the angular distributions is then naturally understood by the size of matter distributions for  $1s$  and  $2s$  orbitals. Since the  $2s$  orbital has a larger mean radius than the  $1s$  orbital, the angular distribution (in  $q$  space) is narrower for the 5 MeV structure. The result indicates that the gap between the  $1p$  and  $2s$  orbitals is about 5 MeV, significantly smaller than the gap between  $1s$  and  $1p$  orbital of about 15 MeV.

In conclusion we have measured the  ${}^6\text{Li}(t, {}^3\text{He}){}^6\text{He}$  reaction at 336 MeV. We have observed a broad asymmetric structure at  $E_x \sim 5$  MeV and another structure at 14.6 MeV, as well as strong peaks for the well-known ground and first excited states in  ${}^6\text{He}$ . The angular distributions show that the structure around 5 MeV is

dominated by the negative parity states with a small mixture of positive parity states in its lower-energy portion. The existence of intruder states at such low energies suggests a quenching of the  $1p-2s$  gap in this nucleus.

We acknowledge S. Van der Werf, for fruitful and invaluable discussions. This work is supported in part by the National Science Foundation under Contract Nos. PHY-9528844 and PHY-9605207.

- a*: Department of Physics, Tokyo Institute of Technology, 2-12-1 O-Okayama, Meguro, Tokyo 152-8551, Japan
- b*: Gesellschaft für Schwerionenforschung (GSI), Planckstr. 1, D-64291 Darmstadt, Germany
- c*: Institut de Physique Nucleaire IN2P3-CNRS, 91406 Orsay, Cedex, France
- d*: Physics Division, Argonne National Laboratory, Argonne IL 60439, USA
- e*: Nuclear Physics Division, Bhabha Atomic Research Center, Trombay, Mumbai 400 085, India

#### References

1. B.V. Danilin *et al.*, *Phys. Rev. C* **55**, R577 (1997);  
B.V. Danilin *et al.*, *Nucl. Phys. A* **632**, 383 (1998)
2. S.N. Ershov *et al.*, *Phys. Rev. C* **56**, 1483 (1997).
3. A. Cobis *et al.*, *Phys. Rev. Lett.* **79**, 2411 (1997).
4. S. Nakayama *et al.*, *Phys. Rev. Lett.* **85**, 262 (2000).
5. J. Jänecke *et al.*, *Phys. Rev. C* **54**, 1070 (1996).
6. I. Daito *et al.*, *Phys. Lett. B* **418**, 27 (1998).
7. B.M. Sherrill *et al.*, *Nucl. Instrum. Methods A* **432**, 299 (1999).
8. T. Nakamura *et al.*, *Phys. Lett. B* **493**, 209 (2000).
9. R. Schaeffer and J. Raynal, DWBA70 code; extended version, J. Comfort.
10. S. Van der Werf *et al.*, *Nucl. Phys. A* **496**, 305 (1989).
11. B.A. Brown, A. Etchegoyen, W.D.M. Rae, and N. S. Godwin, computer code OXBASH, 1984 (unpublished).
12. J. Stevenson *et al.*, *Phys. Rev. C* **37**, 2220 (1988).
13. E. K. Warburton and B. A. Brown, *Phys. Rev. C* **46**, 923 (1992).